RAA 2016 Vol. **16** No. **4**, 53 (6pp) doi: 10.1088/1674–4527/16/4/053
http://www.raa-journal.org *http://iopscience.iop.org/raa*

Research in Astronomy and Astrophysics

Contribution of the Earth's gravitational potential to variations in orbital motion of short-period comets

Valentina M. Chepurova[1], Nelli V. Kulikova[2] and Elena N. Petrovskaya[2]

[1] Sternberg Astronomical Institute, Lomonosov Moscow State University, 13 University Ave., Moscow 119092, Russia; *chep@sai.msu.ru*
[2] Department of Computer Systems, Networks and Technologies, National Research Nuclear University, Moscow Engineering Physics Institute, Institute for Nuclear Power Engineering, Moscow, Russia; *nelvaku@yandex.ru, pen@iate.obninsk.ru*

Received 2014 September 17; accepted 2015 October 16

Abstract We present simulation results on evolution development of orbital motion of short-period comets with the revolution period not exceeding 6–7 years, namely comets 21P/Giacobini–Zinner, 26P/Grigg–Skjellerup and 7P/Pons–Winnecke. The calculations cover the range from the date of the object's discovery to 2100. Variations in the objects' orbital elements under the action of gravity disturbances, taking Earth's gravitational potential into account when the small body approaches, are analyzed. Corrected dates of perihelion passages can be used for scheduling observations.

Key words: comets: individual (21P/Giacobini–Zinner, 26P/Grigg–Skjellerup, 7P/Pons–Winnecke) — meteorites, meteors, meteoroids

1 INTRODUCTION

A system of computational methods (Kulikova & Tischenko 2012) has been developed to study the formation and subsequent evolutional development of meteor complexes that appear in the process of disintegration of small bodies (comets, in particular). The method, based on application of statistical techniques (in particular, the Monte Carlo method), incorporates several modules which implement different algorithms that simulate the eruption of substances from a parent body as well as those that characterize further orbital changes under the action of numerous factors. A module accounting for gravity disturbances is one example. Gravity disturbances are essential for studying motions of celestial bodies in the inner and outer solar system. This factor incorporates the following three components: gravity disturbance in an N-body problem (Everhart 1974); disturbance of a major planet's gravitational potential with the approach of small bodies (Aksenov 1977; Chepurova 1972; Chepurova 1980); disturbance of Earth's gravitational potential with the approach of a small body (Noskov 1970; Kulikova et al. 2010; Kulikova et al. 2011).

Until now, calculation algorithms and graphical presentation of results only permitted taking into account the two first components.

The computer implementation of the last two components includes four problems: transition from elements of a heliocentric orbit of a small body to its planetocentric coordinates; calculation of the intermediate-orbit elements with respect to the approaching planet using planetocentric coordinates; calculation of planetocentric rectangular and cylindrical coordinates at any time using the intermediate-orbit elements obtained in the preceding problem; inverse transformation from a planetocentric orbit to a heliocentric one.

Currently, the system of computational methods we have developed takes many disturbing factors into account (for example, the Poynting–Robertson and Jarkowski–Radzievsky effects, etc.); however, perturbations from the Moon when the small body is approaching the Earth or from planetary satellites when the small body is entering the gravitational spheres of a giant planet have not yet been incorporated.

The paper is structured as follows. Section 2 describes the aims of our study and introduces the three comets considered as individual objects. Section 3 discusses and analyzes the results we obtained. Section 4 deals with a study of perihelion distances of comets in our research program during their life cycles; it also considers positions of the corresponding meteoroid complexes in space with respect to Earth's orbit. We draw our conclusions in Section 5.

2 GOALS, PROBLEMS AND OBJECTS

In this study, we apply a mathematical algorithm that accounts for disturbance of Earth's gravitational potential, which can generate a better approximation. Our calculations have been performed using analytical formulas of the intermediate hyperbolic orbit based on the asymmetric ver-

sion of a generalized problem with two fixed centers that include disturbances of the second and the third harmonics in a series describing the gravitational potential of the central body (Chepurova 2011).

Insofar as the simulated meteoroid complex initially has boundaries dictated by the maximum and minimum deviations in orbital elements of ejected fragments from the parent body's orbit, in the process of its motion, the comet remains within these boundaries. Therefore, three short-period comets with periods of revolution up to seven years are considered as an illustration of this component's impact on the orbital evolution of meteor formations. In view of this, the simulation results on evolutionary development of the comet's motion have been analyzed. The calculated time range is from the date of the first object's observation till 2100. Comets 21P/Giacobini–Zinner, 7P/Pons–Winnecke and 26P/Grigg–Skjellerup have been chosen as objects of investigation. The choice of these objects is primarily based on a large body of evidence that permits the simulation results and observed parameters to be compared. Some results are presented here.

3 DISCUSSION AND ANALYSIS OF RESULTS

Figures 1 and 2 show diagrams which illustrate variations in the primary orbital elements of the program objects within a selected time range and make it possible to draw various conclusions on the motion of objects. The following symbols are used: for comet 26P/Grigg–Skjellerup with (blue diamonds) and without (magenta squares) considering effects of Earth's gravitational potential, comet 7P/Pons–Winnecke with (black triangles) and without (blue crosses) it, and comet 21P/Giacobini–Zinner with (violet asterisks) and without (brown filled circles) it. The minimum and maximum values of these elements are given in Table 1. The elements denoted with an apostrophe are obtained taking account of disturbances from the Earth's gravitational potential. Now we analyze the results obtained for each comet.

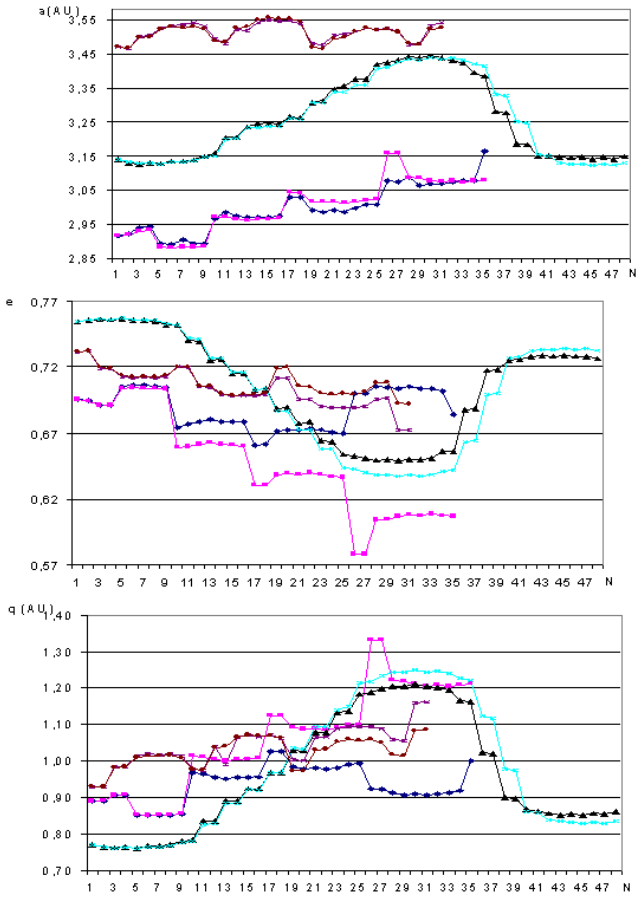

Fig. 1 Variations in the semimajor axis, eccentricity and perihelion distance of cometary orbits within the simulation interval. N is the number of revolutions of the comet. Blue and magenta symbols are for comet Crigg–Skjellerup with and without the effects of Earth's gravitational potential respectively; black and light blue symbols: the same for comet 7P/Pons–Winnecke; violet and brown symbols: the same for comet 21P/Giacobini–Zinner.

Comet 21P/Giacobini–Zinner. This comet was discovered in 1900 and, within the calculation range till 2100, had 31 revolutions. Figure 1 shows the variations in orbital elements (characterizing the form of the orbit) obtained by taking account of disturbances of Earth's gravitational potential and without it for the case of a small body approaching. It can be seen that values of the semimajor axis in 1900–2100 vary episodically and form three pronounced wave-like structures which consist of 2 revolutions with high values of a, 5 revolutions with the highest "wave" and 2 revolutions with a drastic decrease in the semimajor axis. The time intervals are the following: 1913–1919 (rise), 1926–1953 (peak), 1959–1966 (fall); 1972–1979 (rise), 1985–2012 (peak), 2019–2025 (fall); 2032–2038 (rise), 2045–2071 (peak), 2078–2084 (fall). It seems that revolutions 30 and 31 (2091–2097) form the start of the following variation cycle. This structure remains unchanged for both versions of the calculation, and only the numerical values change. Furthermore, in the first and the third bursts, values of the semimajor axis obtained by taking account of disturbances from Earth's gravitational potential are somewhat higher compared to those obtained without it. For the second burst the situation is opposite, i.e. variations in values of the semimajor axis without considering disturbances prevail over those calculated with disturbances taken into account. Values of the semimajor axis obtained without considering these effects are maximum in 1992 and minimum in 2025 during revolutions 15 and 20, respectively. With this effect taken into account, the maximum (revolution 15) and minimum (revolution 28) values are also observed in 1992 and 2078, respectively. In addition, the difference in semimajor axis values calculated in two versions amounts to $\Delta a_{\max} = 0.013939$ AU (revolution 16), $\Delta a_{\min} = 0.000689$ AU (revolution 23) or from 2.07691 million km to 0.1027 million km. The tendency for eccentricity variations is similar and opposite in phase to variations in the semimajor axis. Before 2019, the effect of disturbances from Earth's gravitational potential has lit-

Table 1 Changes in the Orbital Elements

21P/Giacobini–Zinner	7P/Pons–Winnicke	26P/Grigg–Skjellerup
$a_{\max} = 3.5571$ AU (1992) $a'_{\max} = 3.5441$ AU (1992) $a_{\min} = 3.4653$ AU (2025) $a'_{\min} = 3.4772$ AU (2078) $\Delta a_{\max} = 2.0769 \cdot 10^6$ km $\Delta a_{\min} = 0.1027 \cdot 10^6$ km $\Delta e_{\max} = 0.020391$ (2091) $\Delta e_{\min} = 0.000334$ (1959) $\Omega^\circ \in (192 - 198)$ (both versions) $\Delta\Omega \leq 0.1^\circ$ from 2019 (19 rev.) – change of sign $\omega \in (170.8^\circ - 173.85^\circ)$ $\omega' \in (170.40^\circ - 173.15^\circ)$ $\Delta\omega \in (0.03832^\circ 0.17662^\circ)$ 1900–2012 (18th rev.), then till 2084 $\Delta\omega \in (0.45077^\circ - 0.73359^\circ)$ and in 2091, $> 1.5^\circ$ $i \in (29.86^\circ - 33.53^\circ)$ $i' \in (29.87^\circ - 33.66^\circ)$ $\Delta i < 0.05^\circ$ till 2012, then $\leq 0.3^\circ$ $(2025 - 2084)$	$a_{\max} = 3.4396$ AU (1989) $a'_{\max} = 3.4431$ AU (1990) $a_{\min} = 3.1214$ AU (2079) $a'_{\min} = 3.1416$ AU (2078) $\Delta a_{\max} = 4.0798 \cdot 10^6$ km $\Delta a_{\min} = 0.5956 \cdot 10^6$ km $\Delta e_{\max} = 0.02042$ $\Delta e_{\min} = 0.00621$ $\Delta\Omega \leq 0.5^\circ$ till 2045 (39 rev.), then $\leq 2.6^\circ$ (2095, 40–48 rev.) $\omega \in (162.09^\circ - 181.90^\circ)$ $\omega' \in (162.09^\circ - 180.74^\circ)$ $\Delta\omega \leq 0.5^\circ$ till 2021 (35 rev.) $\Delta\omega \leq 0.88^\circ$ till 2051 (40 rev.) and then to 1.2° $i \in (10.83^\circ - 22.21^\circ)$ $i' \in (10.81^\circ - 22.11^\circ)$ $\Delta i \in (0.228^\circ - 0.285^\circ)$ 1–36 rev. $\Delta i \in (1.464^\circ - 3.078^\circ)$ 37–40 rev. (2033–2095)	$a_{\max} = 3.1578$ AU (2050) $a'_{\max} = 3.0867$ AU (2061) $a_{\min} = 2.8808$ AU (1947) $a'_{\min} = 2.8922$ AU (1947) $\Delta a_{\max} = 3.01129 \cdot 10^6$ km $\Delta a_{\min} = 0.61239 \cdot 10^6$ km $\Delta e_{\max} = 0.00155$ $\Delta e_{\min} = 0.08298$ $\Omega^\circ \in (208 - 217)$ (both versions) $\Delta\Omega \leq 0.7^\circ$ (1997, 16 rev.), then decreases to 0.45° (2044, 25 rev.) $\omega,\ \omega' \in (-5^\circ - +7^\circ)$ $\Delta\omega \leq 0.145^\circ$ (9 rev.), in 2002 (17th rev.) – shift to the first quarter $\Delta\omega \approx 0.01^\circ$ $i \in (17.46^\circ - 22.74^\circ - 24.5^\circ)$ $i' \in (17.45^\circ - 20.29^\circ)$ 1–25 rev. $\Delta i \in (0.0036^\circ - 0.0257^\circ)$ till 1961, 9 rev. $\Delta i \in (1.6466^\circ - 1.7001^\circ)$ till 1997, 15 rev. $\Delta i \in (2.3951^\circ - 2.4615^\circ)$ till 2044, 25 rev.

tle influence on the decrease of orbital eccentricity values within the whole calculation period; later on, this effect grows till 2097. The tendency to change the angular elements Ω, ω and i is clearly seen in Figure 2. During the whole simulation period the variations in the longitude of ascending node do not exceed 5° and are within 193°–198° independent of the version of the calculation. The differences between Ω values calculated from both versions do not exceed 0.1 and only starting in 2019 does the sign of $\Delta\Omega$ change in revolution 19. A diagram which illustrates the orbital inclination i acts as a kind of mirror reflecting the above situation for Ω, with the difference that the Ω curves tend to decrease in the simulation interval and the curves of inclination show an increase within $< 4^\circ$.

The diagrams for Ω and i clearly reveal time intervals that show rather smooth moderate variations (revolutions 7–9) and intervals with drastic changes. In the diagrams for ω, we also distinguish three variation episodes, though with more complex behaviors, with peaks for the same years. In 1900–1966 (revolutions 1–11), the values of ω, calculated without taking Earth's gravitational potential into account, turn out to be higher; in 1972–2012 (revolutions 12–18), lower; and in 2019–2097, again higher than those calculated in the case of this considered factor.

Comet 7P/Pons–Winnecke. Considering that this comet was discovered in 1819, the time interval of its investigation turns out to be the longest of the three objects and amounts to 48 orbital revolutions. Figures 1 and 2 show the diagrams of variations in the comet's orbital elements with disturbances (and without them) from Earth's gravitational potential when the comet approaches it. The time intervals are clearly defined when variations in the studied values are insignificant, and the curves are so close that they practically coincide in the diagrams, not necessarily at the beginning of calculations. The largest discrepancy in values is observed at the last stage of calculations, beginning from revolution 35. Accounting for Earth's gravitational potential results in changes of the semimajor axis within (0.004–0.027) AU and of eccentricity within (0.0061–0.02042). The values of angular elements vary as follows: the longitude of ascending node Ω is slightly affected by the potential (by no more than 0.5°); however, beginning with revolution 38, the difference grows and reaches 2.6°. For the argument of perihelion ω, the same pattern is observed before revolution 35 ($\leq 0.5^\circ$); after that it rises to 0.877° (revolutions 35–40), increasing the difference to 1.2° and keeping it to the end of the calculation interval. The orbital inclination i changes minimally from 0.0228° to 0.285° (revolutions 1–35); in revolution 37 it grows to 1.464° and later to 3.078° in revolution 40, staying within the last value to the end of the simulation period.

Comet 26P/Grigg–Skjellerup. Within the calculation interval from the time of its appearance in 1922 till 2100, the comet makes 35 revolutions with evolutionary changes in the orbit. Figures 1 and 2 present variations in the orbital elements determined with disturbances from Earth's gravitational potential taken and not taken into account. Changes in the semimajor axis from the minimum value, 2.8808 AU (1947, revolution 6) to the maximum one, 3.1578 AU (2050, revolution 26), with no account of disturbances, have a certain structure. During revolutions 5–8

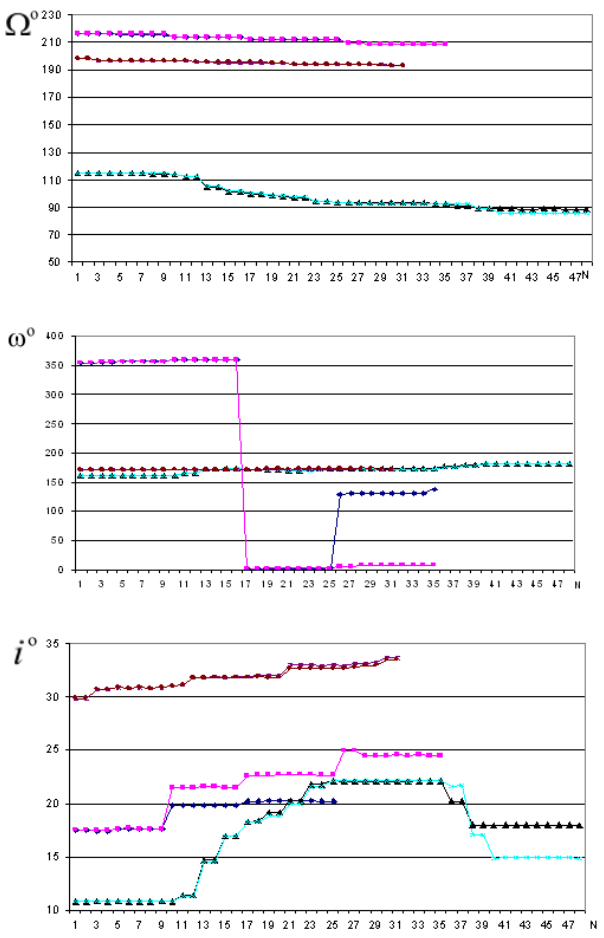

Fig. 2 Variations in the angular elements of cometary orbits within the simulation period. N is the number of revolutions of the comet. The same symbols as in Fig. 1 are used.

there is a relatively gradual increase-decrease in the semimajor axis values; then an abrupt increase occurs which is followed by a drastic fall in 2 revolutions. The considered disturbances by Earth's gravitational potential do not govern variations in this parameter, however, they influence the numerical values. Thus, before 2002 (revolution 16) the value of Δa (the difference in values of the semimajor axis in view of disturbances by Earth's gravitational potential and without them) range within 0.00411–0.02021 AU that corresponds to (0.6–3) million km. Starting in 2008 and to the end of the calculation interval (2100), the influence of the Earth's gravitational potential decreases the semimajor axis. The maximum 3.08867 AU and minimum 2.8922 AU values are observed in 2061 (revolution 28) and in 1947 (revolution 6), respectively. Eccentricity changes in the first 4 revolutions become apparent in the 4th sign after the decimal point, but later this difference increases. During the following 4 revolutions the eccentricity values obtained by taking account of disturbances from Earth's gravitational potential exceed those calculated without them. Beginning in 1961 (revolution 9), the difference rises and gradually grows to the end of the calculation period. In the whole interval studied the longitude of ascending node Ω, the argument of perihelion ω and the inclination of orbit i are characterized by episodic variations in both versions of the simulation. The longitude of ascending node tends to decrease, whereas the argument of perihelion ω and the inclination i increase.

Figure 2 shows the first abrupt change in the values of Ω, ω and i (Ω decreasing, ω, i increasing) since 1961 (revolution 9). For the longitude of ascending node the first noticeable differences in view of disturbances by Earth's gravitational potential appear in 1997 (revolution 16), $\Delta\Omega = 0.66981°$, and gradually decrease to $0.44967°$ (2044, revolution 25). Changes in the argument of perihelion ω in both versions of the simulation are insignificant, i.e. $\leq 0.145°$ (revolution 9); in 2002 (revolution 17), there is a change of ω from the fourth quarter to the first one with a $2.76°$ and $2.75°$ difference from the previous value in view of Earth's gravitational potential and without it, respectively. Like Ω and ω, the values of i change in 1961 and 1997 (revolutions 9 and 16). Later, in the interval from 2002 to 2044, there is a new rise of this value not exceeding $22.74°$. Calculations according to the second version (with disturbances taken into account) result in variations of i only in the form of this parameter's decrease.

Sufficiently interesting are the simulation results which present variations in the perihelion distance during the whole life cycle of the comets studied (Table 2) as well as the spatial position of meteoroid complexes of these comets relative to Earth's orbit projected on the ecliptic plane (Fig. 3).

4 PROGNOSTIC INFERENCE

For comet 21P/Giacobini–Zinner, the differences in numerical values for the perihelion distance in both calculations (Table 2) are insignificant. The system's comet–meteoroid complex is closest to the Earth's orbit in 1926–1933 (Fig. 3a). Intense Draconid meteor showers were actually observed on Earth, especially in 1926. A period of slight variations in the system near the Earth's orbit is observed until 1985.

Since 1985 and to the end of the simulation interval, the comet remains beyond the Earth's orbit. The appearance of meteor showers in the Earth's atmosphere will depend on the width of the meteoroid stream. A close approach will be observed in 2019 and 2025. More spectacular phenomena in the atmosphere might be expected thereafter. From now forth, the comet moves away from the Earth's orbit and, with no increase in its activity, an intense Draconid meteor shower would hardly be observed again before 2100.

Simulated spatial motion of the 7P/Pons–Winnecke meteoroid complex from 1919 to 1983 is presented in Fig. 3b. It appears that in 1921 and 1927, when meteor streams had been registered on the Earth, the meteoroid complex crossed the Earth's orbit moving away from the Sun. According to Table 2, the complex is the most remote

Table 2 Variations in the Perihelion Distance

No.	26P/Grigg–Skjellerup			7P/Pons–Winnicke			21P/Giacobini–Zinner		
	Year	1	2	Year	3	4	Year	5	6
1	1922	0.8889	0.8889	1819	0.7719	0.7719	1900	0.9315	0.9315
2	1927	0.8927	0.8927	1825	0.7657	0.7651	1906	0.9290	0.9292
3	1932	0.9088	0.9069	1830	0.7628	0.7620	1913	0.9837	0.9810
4	1937	0.9091	0.9072	1836	0.7652	0.7639	1919	0.9862	0.9837
5	1942	0.8537	0.8540	1841	0.7620	0.7606	1926	1.0136	1.0092
6	1947	0.8508	0.8511	1847	0.7667	0.7652	1933	1.0194	1.0152
7	1952	0.8533	0.8536	1852	0.7673	0.7654	1939	1.0178	1.0132
8	1957	0.8524	0.8534	1858	0.7704	0.7685	1946	1.0208	1.0161
9	1962	0.8550	0.8558	1863	0.7811	0.7781	1953	1.0134	1.0088
10	1967	0.9670	1.0136	1869	0.7837	0.7807	1959	0.9784	0.9779
11	1972	0.9658	1.0119	1875	0.8340	0.8262	1966	0.9754	0.9748
12	1977	0.9554	1.0044	1880	0.8356	0.8279	1972	1.0383	1.0376
13	1982	0.9513	1.0002	1886	0.8889	0.8834	1979	0.9906	1.0401
14	1987	0.9550	1.0043	1892	0.8898	0.8845	1985	1.0658	1.0657
15	1992	0.9551	1.0057	1898	0.9251	0.9215	1992	1.0720	1.0719
16	1997	0.9575	1.0078	1904	0.9247	0.9211	1999	1.0681	1.0687
17	2003	1.0274	1.1247	1909	0.9700	0.9697	2005	1.0708	1.0696
18	2008	1.0267	1.1235	1915	0.9675	0.9673	2012	1.0635	1.0623
19	2013	0.9827	1.0921	1921	1.0300	1.0368	2019	1.0043	0.9743
20	2018	0.9794	1.0885	1927	1.0286	1.0352	2025	1.0023	0.9727
21	2024	0.9809	1.0901	1933	1.0799	1.0936	2032	1.0655	1.0298
22	2029	0.9770	1.0857	1939	1.0801	1.0934	2038	1.0682	1.0327
23	2034	0.9817	1.0909	1945	1.1340	1.1407	2045	1.0900	1.0535
24	2039	0.9921	1.0970	1951	1.1362	1.1500	2051	1.0962	1.0595
25	2044	0.9934	1.0991	1957	1.1841	1.2147	2058	1.0936	1.0568
26	2049	0.9242	1.3330	1964	1.1890	1.2185	2065	1.0962	1.0589
27	2054	0.9214	1.3321	1970	1.1977	1.2353	2071	1.0891	1.0517
28	2060	0.9113	1.2222	1976	1.2062	1.2422	2078	1.0595	1.0175
29	2065	0.9068	1.2193	1983	1.2032	1.2419	2084	1.0564	1.0146
30	2071	0.9093	1.2092	1989	1.2092	1.2488	2091	1.1593	1.0838
31	2076	0.9059	1.2049	1996	1.2035	1.2437	2097	1.1610	1.0858
32	2081	0.9106	1.2078	2002	1.2013	1.2459			
33	2087	0.9138	1.2032	2008	1.1965	1.2411			
34	2092	0.9175	1.2087	2015	1.1672	1.2271			
35	2098	1.0005	1.2113	2021	1.1632	1.2221			
36				2027	1.0251	1.1220			
37				2033	1.0208	1.1174			
38				2039	0.9007	0.9781			
39				2045	0.8975	0.9753			
40				2051	0.8667	0.8611			
41				2056	0.8632	0.8583			
42				2062	0.8569	0.8381			
43				2068	0.8535	0.8348			
44				2073	0.8553	0.8335			
45				2079	0.8517	0.8295			
46				2084	0.8566	0.8336			
47				2090	0.8552	0.8312			

in revolution 30 (1989–1990) and then the complex begins to approach Earth's orbit.

In 2033, the complex will appear inside Earth's orbit again. Regarding observed eruptive activity of the comet recorded during its passage in 2008 when this comet had changed its luminosity from 18.5 to 15.9, it can be expected that in 2027 and 2033 the meteoroid situation near Earth's orbit will be similar to that observed in 1921–1927 and meteor showers are expected. From now the comet and the whole complex will be in the inner part of Earth's orbit. The tendency for changes in the perihelion distance is similar in both versions of the simulation versions, and the numerical values vary insignificantly.

Since 1922, the tendency to change the perihelion distance (Table 2) and the spatial position (Fig. 3c) for comet 26P/Grigg–Skjellerup and its meteoroid complex has been characterized by a gradual increase in numerical values and a passage from the inner part of Earth's orbit into the outer solar system. It should be noted, however, that consideration of the disturbing action of Earth's gravitational potential slows down this process. So, starting in 1922 the numerical value increases from 0.8889 AU to 1.0274 AU

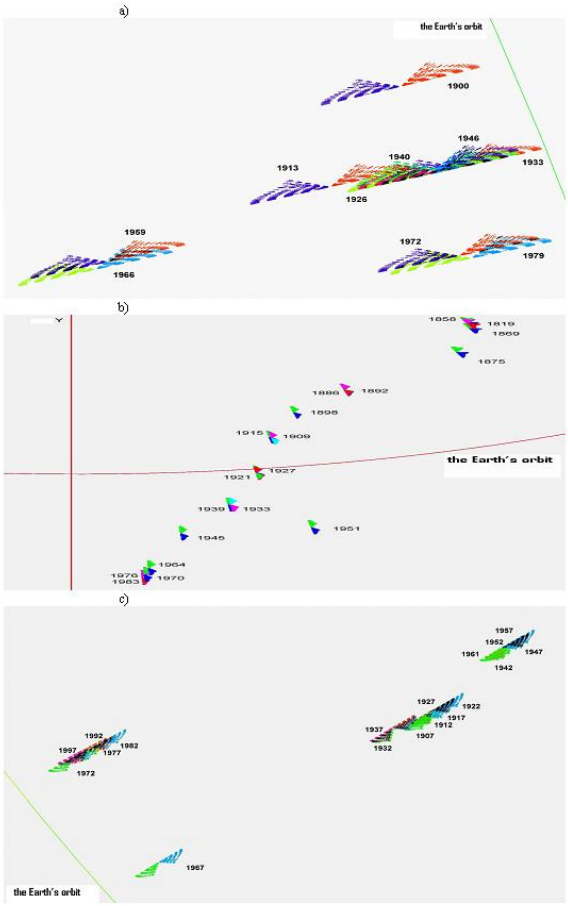

Fig. 3 Spatial position of meteoroid complexes of comets: (a) 21P/Giacobini-Zinner, 1907–1997; (b) 7P/Pons–Winnecke, 1819–1983; (c) 26P/Grigg–Skjellerup, 1900–1979 relative to Earth's orbit projected on the ecliptic plane.

(2003) and later to 1.026 AU (2008) and then falls to 0.917 AU (2092). In revolution 35 (2098), this parameter abruptly rises to 1.0005 AU. Consequently, there is a clearly pronounced pattern, i.e. during 16 revolutions the complex slowly approaches the Earth's orbit from within; in 2003, during revolution 17, it crosses the orbit and remains there during one more revolution. From 2013, during another 16 revolutions, it advances slowly and steadily into the interior of Earth's orbit. However, in 2098, during revolution 35, it suddenly appears almost exactly in Earth's orbit. Since the comet and its meteoroid complex are within Earth's orbit during most of the cycle considered and if the complex itself has an extended structure or covers its own orbit, only weak meteor showers might be observed as Earth's orbit would be crossed by the part of the complex that is most distant from the parent comet. A somewhat different scheme of motion is obtained in simulations without disturbing action. Before 1967, the complex is inside Earth's orbit, then abruptly crosses it, and till 1997 (16 revolutions), it is near Earth's orbit exteriorly.

From 2003 to the end of the calculation interval (2098), the complex is gradually moving away from Earth's orbit, with the abrupt maximum in distance occurring in 2049–2054.

5 CONCLUSIONS

Consideration of the disturbing action of Earth's gravitational potential on the orbital motion of studied comets also changes the particular dates of perihelion passage by the objects. The observation dates of meteor showers identified with them are also influenced. According to the calculated data obtained in different years, the value of the change can vary from a day to half a year; e.g. for comet 21P/Giacobini–Zinner, it can vary from one day in 1919, 1999, 2078 and 2084 to 38 days in 1959; in other cases, changes up to 3–5 months can happen. It is worth noting that primary changes in the orbital elements of comets with $5 < P < 7$ years appear at the times of Saturn's and Jupiter's resonance (2:5), i.e. at 59-year time intervals. The degree of their approach governs the amount of orbital element variations. This pattern is clearly seen for comets 21P/Giacobini–Zinner and 7P/Pons–Winnecke. It is less evident for comet 26P/Grigg–Skjellerup, probably due to a different orientation of its orbit (ω). The dates of close approaches for these comets determined by other authors (Zausaev 2008) confirm our results.

Acknowledgements The authors are grateful to the anonymous referee for helpful suggestions that permitted us to improve the original manuscript.

References

Aksenov, E. P. 1977, Theory of the Earth Artificial Satellite Motion (Moskva: Nauka), 364

Chepurova, V. M. 1972, in The Motion, Evolution Orbits, and Origin of Comets, eds. G. A. Chebotarev, E. I. Kazimirchak-Polonskaia, & B. G. Marsden (Dordrecht, Reidel), 62

Chepurova, V. M. 1984, BITA, 15, 5, 288

Chepurova, V. M., & Kulikova N. V. 2011, SibGAU Vestnik, Krasnoyarsk, 6, 83, *www.vestnik.sibsau .ru/images/stories /Statii/2011/6_39_2011_1.pdf*

Everhart, E. 1974, Celestial Mechanics and Dynamical Astronomy, 10, 35

Kulikova, N. V., Polyakov, N. V., & Chepurova, V. M. 2010, Radiotekhnika (Kharkov), 160, 82

Kulikova, N. V., Polyakov, N. V., & Chepurova, V. M. 2011, Astronomical and Astrophysical Transactions, 27, 105

Kulikova N.V., & Tischenko V.I., 2012, RosNou Vestnik, 4, 34, *vestnik-rosnou.ru/node/150*

Noskov, B. N. 1970, Sosht, 159, 14

Zausaev, A. F., & Zausaev, A. A. 2008, Mathematical Simulation of the Orbital Evolution of the Solar System Small Bodies (Moscow: Mashinostroenie), 250